# Photophysics of [Pt{4-($o$-tolyl)isqbipy}Cl]SbF$_6$, where 4-($o$-Tolyl)isqbipy is the New 4-($o$-Tolyl)-6-(3″-isoquinolyl)-2,2′-bipyridyl Ligand

John S. Field[a], Jan-André Gertenbach[a], Deogratius Jaganyi[a], David R. McMillin[b], Aishath Shaira[a], and David J. Stewart[b]

[a] School of Chemistry, University of KwaZulu-Natal, Private Bag X01, Pietermaritzburg, 3201, South Africa
[b] Department of Chemistry, Purdue University, West Lafayette, Indiana, 47907-1393, USA

Reprint requests to Prof. John Field. Fax: +27-33-2605009. E-mail: fieldj@ukzn.ac.za

The synthesis and characterisation of the 4-($o$-tolyl)-6-(3″-isoquinolyl)-2,2′-bipyridyl [4-($o$-tolyl)isqbipy] ligand is described. A single-crystal X-ray structure determination shows that it adopts a *trans-trans* conformation about the interannular bonds linking the central pyridine ring to the outer pyridine ring and the isoquinolyl moiety. The $o$-tolyl group is twisted by an angle of 51.7° out of the plane of the central pyridine ring. The synthesis and characterisation of the [Pt{4-($o$-tolyl)isqbipy}Cl]SbF$_6$ complex is described. The absorption spectrum of the complex measured in acetonitrile exhibits MLCT bands at 362 and 393 nm, as well as intraligand $\pi$-$\pi^*$ absorptions in the 200–350 nm range; the MLCT bands are shifted significantly to higher energy when compared to those recorded for the parent trpy complex, *viz.* [Pt{4′-($o$-tolyl)trpy}Cl]SbF$_6$, where trpy is 2,2′:6′,2″-terpyridine. Similarly, the $^3$MLCT emission measured for the 4-($o$-tolyl)isqbipy complex in a 1:1 CH$_2$Cl$_2$/CHCl$_3$ solution is blue-shifted with respect to the emission spectrum recorded for the 4′-($o$-tolyl)trpy complex. We attribute the higher energy MLCT absorption and emission for the 4-($o$-tolyl)isqbipy complex to a significantly higher energy for its $\pi^*$-LUMO than for that of the 4′-($o$-tolyl)trpy complex. Emission spectra of the title compound have also been measured in a low-temperature 1:5:5 (v/v) DMF/methanol/ethanol (DME) glass as a function of concentration. These spectra show that aggregation of the complex occurs at rather low concentrations of 5–10 $\mu$M, probably to dimers. Variable-temperature emission spectra recorded on a solid sample of [Pt{4-($o$-tolyl)isqbipy}Cl]SbF$_6$ comprise relatively narrow asymmetric bands whose maxima are shifted to the red as the temperature is lowered: specifically $\lambda_{em}$(max) is 641 nm at r. t. ($\tau = 235$ ns) and 676 nm at 77 K ($\tau = 1.36$ $\mu$s). Temperature-dependent emission of this type is typical of a metal-metal-to-ligand charge transfer (MMLCT) excited state that has its origin in $d_{z^2}$(Pt)-$d_{z^2}$(Pt) orbital interactions in the crystal.

*Key words:* Isoquinolyl-bipyridyl Ligand, Crystal Structure, Platinum Complex, Photophysics

## Introduction

In a seminal 1993 report Che and co-workers showed that complexes of platinum(II) with the 2,2′:6′,2″-terpyridyl (trpy) ligand possess interesting photophysical properties [1]. The focus of their work was the absorption and emissive properties of the [Pt(trpy)Cl]$^+$ chromophore as the triflate salt, both in fluid solution and in the solid state [1]. In a 1994 paper, McMillin and co-workers reported absorption and luminescence data for a series of complexes with the formula [Pt(trpy)$X$]$^+$ ($X$ = Cl, NCS, OMe or OH) [2]. Subsequently, in a 1995 report, Gray and co-workers demonstrated the importance of intermolecular stacking interactions in determining the luminescence prop-

erties of salts of the [Pt(trpy)Cl]$^+$ chromophore, in a concentrated glass and in the solid state [3]. Since these three early reports, researchers have aimed to tune the photophysical properties of complexes of this type, both in solution and in the solid state. One approach has been to study the effect of changing the co-ligand on the photophysical properties of the complex. The effect is dramatic when the weak-field chloride ion is replaced with a strong-field ligand, such as the hydroxide [2] or cyanide anion [4, 5]. However, a more widely adopted approach has been to modify the trpy ligand itself, either through direct substitution of a pyridine ring with electron withdrawing or donating groups [6–9], or by introducing an aromatic ring substituent in the 4′-position of the trpy ligand *i. e.* the *para* position of
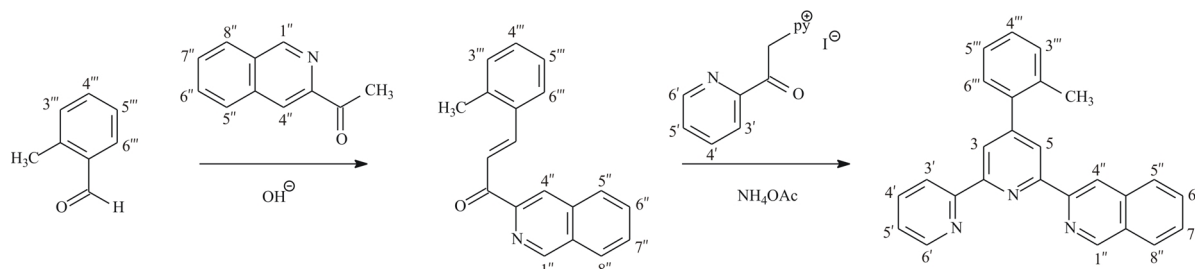
Scheme 1. Route used for the synthesis of 4-(*o*-tolyl)-6-(3″-isoquinolyl)-2,2′-bipyridine.

the central pyridine ring [1, 10 – 21]. Note that the ring substituent in the 4′-position may itself be substituted in such a way as to render the cation non-planar, and that this can have a dramatic effect on how the cations are arranged in the solid state, and hence on the solid-state photophysical properties of the material [17 – 21].

It is against this background that we report here a ligand with a trpy core structure, but where one of the outer pyridine rings has been transformed into an isoquinolyl moiety, specifically the 4-(*o*-tolyl)-6-(3″-isoquinolyl)-2,2′-bipyridine [4-(*o*-tolyl)isqbipy] ligand. We wished to establish the effect of replacing an outer pyridine ring with an isoquinolyl moiety on the photophysical properties of the corresponding platinum(II) complex, in this case [Pt{4-(*o*-tolyl)isqbipy}Cl]SbF$_6$. Note that the ligand is new: in fact, there are no previous reports of the synthesis and characterisation of any ligand containing an iso-quinolylbipyridyl core.

**Results and Discussion**

The synthesis of the 4-(*o*-tolyl)isqbipy ligand followed the Kröhnke method [22] and is illustrated in Scheme 1. The first step is an aldol condensation between 3-acetylisoquinoline and *o*-tolualdehyde that affords, after work-up, a pale-yellow solid characterised as 1-(3′-isoquinolyl)-3-(*o*-tolyl)-prop-2-en-1-one. The latter is then reacted with *N*-{1-(2′-pyridyl)-1-oxo-2-ethyl}pyridinium iodide in the presence of ammonium acetate in a ring cyclisation step to afford 4-(*o*-tolyl)-6-(3″-isoquinolyl)-2,2′-bipyridine. The ligand was re-crystallised from warm ethanol as colourless needles with a final yield for the pure product of 34 %. Details of the elemental analysis and spectroscopic characterisation of the ligand are given in the Experimental Section, and the crystal structure is described below.

In order to synthesise [Pt{4-(*o*-tolyl)isqbipy}Cl]-SbF$_6$ the same approach was used as that previ-

ously employed for the synthesis of the trpy analogue *i. e.* [Pt{4′-(*o*-tolyl)trpy}Cl]SbF$_6$ [17]. Thus, [Pt(PhCN)$_2$Cl$_2$] was first reacted with AgSbF$_6$ in refluxing acetonitrile, the AgCl that formed filtered off, and the 4-(*o*-tolyl)isqbipy ligand added to the reaction mixture, finally affording the product as a bright-red microcrystalline solid in a yield of 94 %. Characterisation of [Pt{4-(*o*-tolyl)isqbipy}Cl]SbF$_6$ was by means of elemental analysis for % C, H and N, as well as by infrared, $^1$H and $^{13}$C NMR spectroscopy. Unfortunately, despite repeated attempts, it was not possible to grow single crystals suitable for an X-ray diffraction study.

*Crystal structure of 4-(o-tolyl)-6-(3″-isoquinolyl)-2,2′-bipyridine*

Single crystals of the ligand were grown by slow evaporation of a concentrated solution of the compound in 95 % ethanol. A perspective view of the molecule is given in Fig. 1. All the bond lengths and
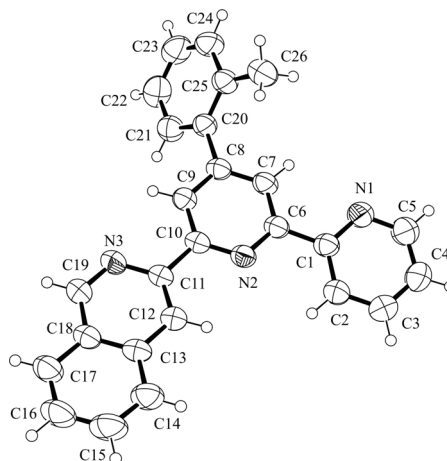


Fig. 1. ORTEP view of 4-(*o*-tolyl)-6-(3″-isoquinolyl)-2,2′-bipyridine drawn with 50 % probability ellipsoids. Hydrogen atoms are drawn as small spheres of arbitrary radius.

angles are as expected. The two pyridyl rings and the isoquinolyl moiety adopt a near planar *transoid* configuration about the interannular C–C bonds, the same configuration as that adopted by 2,2′:6,2″-terpyridine [23], 4′-phenyl-2,2′:6,2″-terpyridine [24] and 4′-[2-(trifluoromethyl)phenyl]-2,2′:6,2″-terpyridine [25]. The *o*-tolyl group is twisted out of the plane of the central pyridine ring, as reflected by a C7–C8–C20–C25 torsion angle of 51.7°. This out-of-plane twist follows from the need to minimise steric repulsions between the *ortho*-methyl group and the hydrogen atom bonded to carbon atom C7 of the central pyridine ring (Fig. 1). The equivalent torsion angles for 4′-phenyl-2,2′:6,2″-terpyridine and 4′-[2-(trifluoromethyl)phenyl]-2,2′:6,2″-terpyridine are 10.9 and 69.2° respectively [24, 25]. The value for the former ligand is lower because the 4′-phenyl ring is unsubstituted (*i. e.* less steric repulsion) while the larger value for the latter ligand is due to the steric demands of a very bulky trifluoromethyl group in the *ortho*-position of the phenyl ring [25]. A substantial twist around the interannular bond linking the central pyridine ring to the *o*-tolyl group clearly renders the 4-(*o*-tolyl)isqbipy ligand non-planar. We discuss below the implications of this for the likely stacking of the cations in solid [Pt{4-(*o*-tolyl)isqbipy}Cl]SbF$_6$, and for the photophysical properties of the material.

### Photophysical properties of [Pt{4-(o-tolyl)isqbipy}Cl] SbF$_6$

We start with the absorption spectrum of [Pt{4-(*o*-tolyl)isqbipy}Cl]SbF$_6$ measured in acetonitrile. This is shown in Fig. 2 along with the absorption spectra of the closely related trpy complex, [Pt{4′-(*o*-tolyl)trpy}Cl]SbF$_6$. The relatively intense absorption bands in the high energy 200–350 nm region are assigned to intraligand $\pi$-$\pi^*$ transitions by analogy with assignments made for many other terpyridyl (or terpyridyl-like) complexes of platimum(II) [1–21, 26–28]. More interesting are the somewhat less intense bands at wavelengths > 350 nm that are usually assigned as metal-to-ligand charge transfer (MLCT) bands [1–21, 26–28]. For the 4′-(*o*-tolyl)trpy complex there are two such bands, at 380 and 400 nm, while for the 4-(*o*-tolyl)isqbipy complex the corresponding bands occur at 362 nm, and as a shoulder at 393 nm. Clearly, there is a shift to higher energy for the MLCT transitions when an outer pyridine ring in the 4′-(*o*-tolyl)trpy ligand is replaced by the iso-
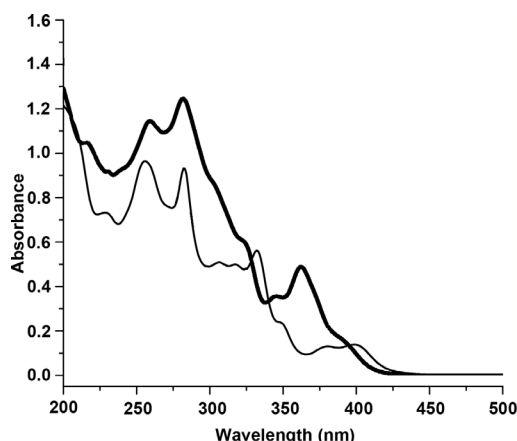


Fig. 2. Absorption spectra measured in acetonitrile for [Pt{4′-(*o*-tolyl)trpy}Cl]$^+$ (thin line) and [Pt{4-(*o*-tolyl)-isqbipy}Cl]$^+$ (thick line).

quinolyl moiety to give the 4-(*o*-tolyl)isqbipy ligand. To help explain this blue shift we refer to a paper by Balzani and co-workers [29]. They report a similar blue shift in the MLCT absorption bands when the 2,2′-bipyridyl (bipy) ligands in [Ru(bipy)$_3$]$^{2+}$ are replaced by 2,2′-bisisoquinoline (*i*-biq) ligands to afford the [Ru(*i*-biq)$_3$]$^{2+}$ complex [29]. The reason given is that the $\pi^*$-LUMO orbital lies at a higher energy in *i*-biq than in bipy, probably due to a smaller localisation of the $\pi^*$-LUMO orbital on the nitrogen atoms of the former ligand [29]. We presume that a similar explanation applies here, *i. e.* the blue shift is the result of a higher energy for the $\pi^*$-LUMO of the 4-(*o*-tolyl)isqbipy ligand, as compared to the energy of the $\pi^*$-LUMO for the 4′-(*o*-tolyl)trpy ligand. Of course, any difference in the energies of the *d*-orbital HOMOs for the two complexes would also play a role in determining the HOMO-LUMO gap and hence the energy of the MLCT absorption. However, any such difference is likely to be very small because the $\sigma$-donor properties of the 4′-(*o*-tolyl)trpy and 4-(*o*-tolyl)isqbipy ligands are expected to be very similar.

The [Pt{4-(*o*-tolyl)isqbipy}Cl]$^+$ complex is non-emissive in acetonitrile; however, we were able to record an emission spectrum, albeit with rather weak bands, in a 1 : 1 CH$_2$Cl$_2$/CHCl$_3$ solution. This is shown in Fig. 3 together with the emission spectrum of the parent [Pt{4′-(*o*-tolyl)trpy}Cl]$^+$ complex for comparison purposes. The emission band profile for both complexes is consistent with a $^3$MLCT assignment, *i. e.* the envelope of vibronic structure shows a pattern of monotonically decreasing intensity [1, 4, 5, 13, 26].
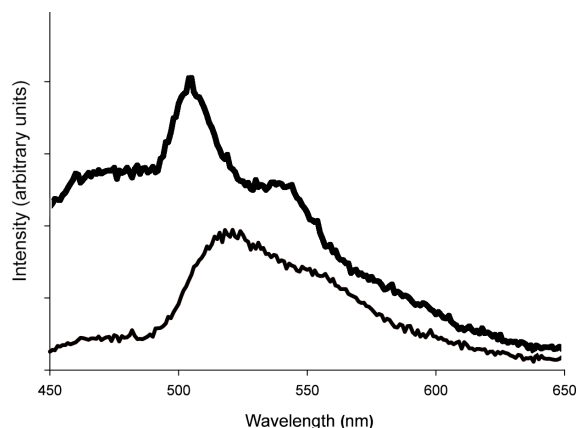
Fig. 3. Degassed emission spectra measured in 1 : 1 CH$_2$Cl$_2$/CHCl$_3$ for [Pt{4'-(*o*-tolyl)trpy}Cl]$^+$ (thin line, $\lambda_{ex}$ = 411 nm) and [Pt{4-(*o*-tolyl)isqbipy}Cl]$^+$ (thick line, $\lambda_{ex}$ = 410 nm).



Fig. 4. Concentration-dependent emission spectra of [Pt{4-(*o*-tolyl)isqbipy}Cl]$^+$ recorded in a 1 : 5 : 5 (v/v) DMF/methanol/ethanol (DME) glass at 77 0K, $\lambda_{ex}$ = 400 nm. Spectra intensities have been matched at 500 nm.

The 0-0 and 0-1 progressions occur at 505 and *ca.* 540 nm for the 4-(*o*-tolyl)isqbipy complex, and at the longer wavelengths of 515 and *ca.* 550 nm for the 4'-(*o*-tolyl)trpy complex. Thus, there is a clear shift to higher energy for the emission by the 4-(*o*-tolyl)isqbipy complex. This is to be expected if, as discussed, the $\pi^*$-LUMO for the 4-(*o*-tolyl)isqbipy complex is higher in energy than that for the 4-(*o*-tolyl)trpy complex. Attempts were also made to measure emission lifetimes for the two complexes in 1 : 1 CH$_2$Cl$_2$/CHCl$_3$, but these were unsuccessful because the lifetimes are so short, specifically less than the detection limit of 10 ns for our instrument. This can be attributed to the presence of low-lying *d-d* excited states that effectively quench the emission [26].

We have also recorded emission spectra of solutions of different concentrations of [Pt{4-(*o*-tolyl)isqbipy}-Cl]$^+$ in a 1 : 5 : 5 (v/v) DMF/methanol/ethanol (DME) glass at 77 K (Fig. 4) [30]. At the lowest concentration of 0.2 $\mu$M, bands at *ca.* 500 and 540 nm are observed, essentially matching those observed in the fluid solution spectrum (Fig. 3). However, at the higher concentrations of 5.0 and 10 $\mu$M a new peak develops at *ca.* 585 nm. This peak is unlikely to form part of the structured emission of the [Pt{4-(*o*-tolyl)isqbipy}Cl]$^+$ monomer, in view of its relatively high intensity (especially at the higher concentration) and the change in band shape – the 585 nm peak is very broad. Most likely it is due to aggregate formation of the type previously observed in concentrated glass solutions of trpy complexes of platinum(II) [3, 11, 31]. However, its position at 585 nm suggests rather weak in-
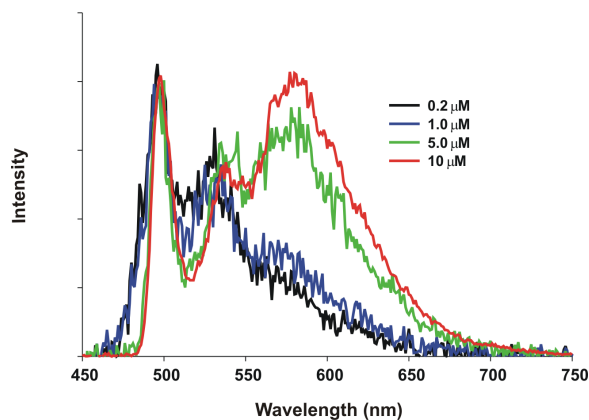
termolecular interactions in the aggregate and/or a lower aggregate, perhaps a dimer. For comparison, aggregate formation in concentrated glass solutions of [Pt(trpy)Cl]$^+$ and [Pt{4'-(Ph)trpy}Cl]$^+$ is evidenced by emission at wavelengths longer than 600 nm [3, 11]; similarly, for the guanidine anion (Gua) bridged dimer [Pt$_2$(trpy)$_2$(Gua)]$^{2+}$ (in which there is only a weak Pt$\cdots$Pt interaction) an emission maximum of 620 nm has been measured in acetonitrile [32]. The intermolecular interactions in the aggregate may be weak, but it is also true that aggregation occurs at rather low concentrations of $\leq$ 10 $\mu$M. To illustrate this behaviour we refer again to the [Pt(trpy)Cl]$^+$ and [Pt{4-(Ph)trpy}Cl]$^+$ cations. For the former, the onset of new peaks due to aggregate formation in a glass only occurs at concentrations of $>$ 10 $\mu$M [3]; for the latter, new peaks due to aggregate formation only appear at concentrations of $>$ 20 $\mu$M [11]. In both these systems the cation is planar [3, 11] whereas the [Pt{4-(*o*-tolyl)isqbipy}Cl]$^+$ cation must be non-planar because of the out-of-plane twist of the *o*-tolyl group (Fig. 1). Intuition suggests that aggregates in the glass will form more easily for planar rather than non-planar systems and, therefore, aggregate formation by the non-planar [Pt{4-(*o*-tolyl)isqbipy}Cl]$^+$ cation at such low concentrations was initially unexpected. This view changes, however, when the solid-state luminescence and likely crystal structure of [Pt{4-(*o*-tolyl)isqbipy}Cl]SbF$_6$ are considered (see the discussion below).

The bright-red [Pt{4-(*o*-tolyl)isqbipy}Cl]SbF$_6$ complex luminesces strongly in the solid state. Fig. 5 shows the emission spectra recorded for an
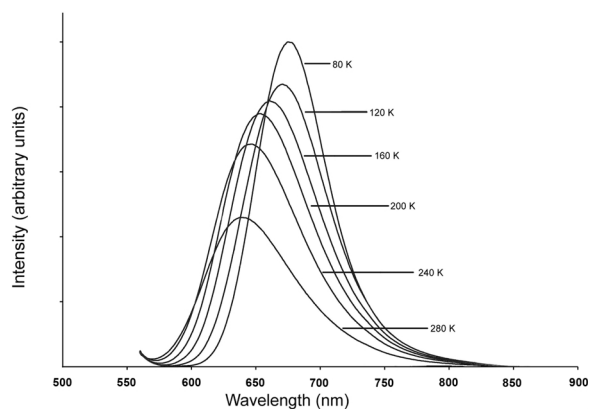
Fig. 5. Variable-temperature emission spectra recorded on a microcrystalline sample of [Pt{4-(*o*-tolyl)isqbipy}Cl]SbF$_6$, $\lambda_{\mathrm{ex}} = 400$ nm.

analytically pure powder sample as a function of temperature in the range 280 to 80 K; we have also measured emission spectra and lifetimes at r. t. and 77 K. At r. t. the spectrum consists of a single asymmetric band centred at 641 nm ($\tau = 135$ ns) with a fwhm (full-width-at-half-maximum) value of 2060 cm$^{-1}$. On reducing the temperature this band increases in intensity, systematically shifts to longer wavelengths reaching 676 nm at 77 K and, at the same time, becomes narrower (fwhm = 1430 cm$^{-1}$; $\tau = 1.36$ $\mu$s at 77 K). These features are diagnostic for $^3$MMLCT emission, *i. e.* emission that originates from a $d\sigma^*$-$\pi^*$(isqbipy) excitation where the $d\sigma^*$ orbital is formed by overlap of $d_{z^2}$-orbitals on adjacent Pt atoms [1, 3, 17 – 21]. With this assignment the red-shift on cooling is easily explained in terms of a lattice contraction that leads to a shortening of the Pt⋯Pt distance that separates neighbouring Pt atoms; this allows for stronger $d_{z^2}$(Pt)-$d_{z^2}$(Pt) orbital interactions and leads to a closing of the HOMO-LUMO energy gap and a concomitant lowering of the energy of the emission [1, 17 – 21, 33 – 35]. Interestingly, the red-shift of 35 nm for a temperature drop from r. t. to 77 K is quite small when compared to red-shifts recorded for similar complexes over the same temperature range, *e. g.* $\Delta\lambda_{\mathrm{em}}$(max) is 57 nm for the trpy analogue [Pt{4′-(*o*-tolyl)trpy}Cl]SbF$_6$ [17] and 70 nm for [Pt(trpy)(NCS)]SbF$_6$ [33].

As already stated, we have not been able to grow single crystals of the title compound, [Pt{4-(*o*-tolyl)isqbipy}Cl]SbF$_6$. However, the photophysical data obtained in the solid state allow some inferences to be made regarding its likely crystal structure. First

is that the [Pt{4-(*o*-tolyl)isqbipy}Cl]$^+$ cations must be stacked in the crystal such that there are metallophilic Pt⋯Pt interactions: were this not the case, $^3$MMLCT emission would not be observed. Of course, without a crystal structure determination, the precise nature of the metallophilic interactions is uncertain. Nevertheless, it is useful to consider the crystal structure of the trpy ligand analogue, [Pt{4′-(*o*-tolyl)trpy}Cl]SbF$_6$ – in this case there is an extended chain of equally-spaced and interacting Pt atoms in the crystal [17]. As we have previously argued, this extended chain structure of Pt atoms is favoured because the out-of-plane twist of the *o*-tolyl group effectively "locks" adjacent cations into a head-to-tail conformation with closely-spaced Pt atoms [17]. Thus, simply from the steric point of view, the same should apply to the cations in crystals of [Pt{4-(*o*-tolyl)isqbipy}Cl]SbF$_6$ – after all, there must be a substantial out-of-plane twist of the *o*-tolyl group in the [Pt{4-(*o*-tolyl)isqbipy}Cl]$^+$ cation, as found for the free ligand (Fig. 1). We therefore presume that there is an extended chain of Pt atoms in crystals of [Pt{4-(*o*-tolyl)isqbipy}Cl]SbF$_6$, but we cannot be certain whether the Pt atoms are equally spaced or whether the stack comprises a series of dimers [1 – 3, 17, 36] or even tetramers [11, 21]. However, as already noted, the response of the wavelength of the emission maximum to changes in temperature is relatively small – only 35 nm over the temperature range of r. t. to 77 K, as compared to 57 nm for [Pt{4′-(*o*-tolyl)trpy}Cl]SbF$_6$ [17]. The implication is that cooling crystals of [Pt{4-(*o*-tolyl)isqbipy}Cl]SbF$_6$ does not lead to large changes in the Pt⋯Pt distances and, on this basis, an oligomer structure seems more likely.

## Concluding Remarks

When the 4′-(*o*-tolyl)trpy ligand is modified to give the 4-(*o*-tolyl)isqbipy ligand the important electronic change is that the energy of the $\pi^*$-LUMO increases significantly. This has as a result that both the $^1$MLCT absorption and the $^3$MLCT emission occur at significantly higher energies for the [Pt{4-(*o*-tolyl)isqbipy}Cl]$^+$ complex, as compared to the [Pt{4′-(*o*-tolyl)trpy}Cl]$^+$ complex. There is also a dramatic effect on the relative reactivities of the two complexes, with the former undergoing substitution reactions far more slowly than the latter [37]. This can be ascribed to the fact that the 4-(*o*-tolyl)isqbipy ligand is a weaker $\pi$-acceptor ligand than the 4′-(*o*-tolyl)trpy ligand [37]. Finally, this work confirms that by sub-

stituting an *o*-tolyl group in the 4′-position of the trpy ligand, or in the 4-position of the isqbipy ligand, the cationic complexes are prevented from sliding past each other, so promoting stacking, both in a concentrated glass solution and in the solid state.

## Experimental Section

### General

Absolute ethanol (99.8 %, Merck) was used as supplied, as was the acetonitrile from Aldrich (99.93+ %, HPLC grade). Other organic solvents and reagents were from Aldrich and used as received except for the ammonium acetate which was dried in a vacuum desiccator over P$_2$O$_5$ for several days prior to use. The methyl-3-isoquinoline carboxylate (98 %) and *ortho*-tolualdehyde (98 %) were purchased from Aldrich and used without further purification. The *N*-{1-(2′-pyridyl)-1-oxo-2-ethyl}pyridinium iodide was prepared by a modification of the Kröhnke method [22]. The method used for the preparation of 3-acetylisoquinoline is a slight modification of the method of Sauvage and co-workers [38] and is described below. [Pt(Ph(CN)$_2$Cl$_2$] (99 %) and AgSbF$_6$ (98 %) were purchased from Strem Chemicals and also used as received (but stored in a desiccator prior to use).

### Instrumentation

Microanalyses for % C, H and N were performed in the Microanalytical Laboratory of the Department of Chemistry, University of Durham, United Kingdom. $^1$H NMR and $^{13}$C NMR spectra were recorded on a Bruker Avance 500 MHz spectrometer, at 298.15 K using Si(CH$_3$)$_4$ as the reference for the chemical shifts. Infrared spectra were recorded from KBr discs on a Perkin Elmer Spectrum One FTIR spectrophotometer. Mass determinations were made using electrospray ionisation mass spectroscopy (ESIMS) with a Hewlett-Packard HP5988A spectrometer equipped with a quadrupole mass filter. UV/Vis absorption spectra were recorded on a Varian CARY 100 Bio spectrophotometer. The emission spectrophotometer was a Varian Cary Eclipse fluorimeter equipped with a R3896 phototube. For the variable-temperature emission measurements the cryostat was an Oxford Instruments DN1704 liquid-nitrogen-cooled system complete with an Oxford Instruments temperature controller. See previous work for a description of the nitrogen-pumped dye laser and associated equipment used for lifetime determinations [39]. The method for determining lifetimes has been described previously [40].

### Syntheses

### 3-Acetylisoquinoline

A mixture of methyl-3-isoquinolinecarboxylate (2.01 g, 10.7 mmol) and anhydrous ethylacetate (3.42 mL,

14.0 mmol) in benzene (35.0 mL) was added to sodium ethoxide (0.729 g, 10.7 mmol) in dry benzene (35 mL) with constant stirring. The resulting mixture was refluxed with stirring for 24 h. The mixture was then cooled and poured into a solution of sodium hydroxide (0.429 g, 10.7 mmol) in water (15 mL). The light-yellow solid that formed was filtered off, and water (40 mL) was added to the filtrate. After separation of the phases, the benzene layer was washed with water, and the combined aqueous layers were extracted with ether (3 × 30 mL). The combined organic layers were evaporated and combined with the light-yellow solid. This was then refluxed in hydrochloric acid (32 mL, 4 M) for 2 h. After cooling, the mixture was made basic with sodium carbonate, the organic layer was extracted with ether (3 × 30 mL) and dried over sodium sulfate. Removal of solvent and drying gave the 3-acetylisoquinoline as a pale-yellow solid. Yield: 1.20 g (66 %). – M. p. 88.5 – 89.0 °C. – IR: $v$ (CO) = 1689 cm$^{-1}$. – $^1$H NMR (400 MHz, CDCl$_3$): $\delta$ = 9.21 (1H, s, H$^{1''}$), 8.50 (1H, s, H$^{4''}$), 7.99 – 8.09 (2H, dd, H$^{8'',6''}$), 7.73 – 7.80 (2H, m, H$^{5'',7''}$), 2.84 (3H, s, CH$_3$).

### *1-(3′-Isoquinolyl)-3-(o-tolyl)-prop-2-en-1-one*

*ortho*-Tolualdehyde (0.459 g, 3.79 mmol) and 3-acetyl-isoquinoline (0.649 g, 3.79 mmol) were dissolved in absolute ethanol (15 mL) and cooled to 0 °C. Sodium hydroxide (4 mL, 1.0 M) was added drop-wise and the reaction mixture stirred at 0 °C for 3 h. The pale-yellow product was precipitated with ice. The precipitate was filtered, washed with 50 % aqueous ethanol and dried *in vacuo*. Yield: 0.97 g (94 %). – M. p. 144.1 – 144.8 °C. – IR: $v$ (CO) = 1664 cm$^{-1}$. – $^1$H NMR (500 MHz, CDCl$_3$): $\delta$ = 9.37 (1H, s, H$^{1''}$), 8.67 (1H, s, H$^{4''}$), 8.38 (1H, $^3J_{HH}$ = 15.78 Hz, *CH*CO), 8.34 (1H, $^3J_{HH}$ = 15.99 Hz, *CH*Ar), 8.09 (2H, m, H$^{8'',6'''}$), 7.91 (1H, d, H$^{6''}$), 7.80 (2H, m, H$^{5'',7''}$), 7.24 – 7.34 (3H, m, H$^{3''',4''',5'''}$), 2.56 (3H, s, CH$_3$).

### *4-(o-Tolyl)-6-(3″-isoquinoyl)-2,2′-bipyridine*

A mixture of 1-(3-isoquinoyl)-3-(o-tolyl)-prop-2-en-1-one (0.892 g, 3.26 mmol), *N*-{1-(2′-pyridyl)-1-oxo-2-ethyl}-pyridinium iodide (1.06 g, 3.26 mmol) and ammonium acetate (16.2 g, excess) was heated to reflux in absolute ethanol (10 mL) for 70 min. On cooling, the resultant precipitate was filtered and washed with 50 % aqueous ethanol. The impure product was then washed with ethanol (95 %), leaving an off-white solid on the frit. The product was re-crystallised from ethanol (95 %) and dried *in vacuo*, to give colourless needle-like crystals. Yield: 0.410 g (34 %). – M. p. 150.2 – 150.7 °C. Anal. for C$_{26}$H$_{19}$N$_3$: calcd. C 83.6, H 5.1, N 11.3; found C 84.1, 5.2, 11.4. – $^1$H NMR (500 MHz, CDCl$_3$): $\delta$ = 9.37 (1H, s, H$^{1''}$), 9.07 (1H, s, H$^{4''}$), 8.77 (1H, d, H$^5$), 8.74 (1H, dd, H$^3$), 8.62 (1H, d, H$^{3'}$), 8.49 (1H, d, H$^{6'}$), 8.08 (2H, t, H$^{8'',4'}$), 7.95 (1H, m, H$^{6''}$), 7.77 (1H, m, H$^{5''}$),

7.66 (1H, m, H$^{7''}$), 7.42 (1H, d, H$^{6'''}$), 7.38 (1H, m, H$^{5'}$), 7.33 (3H, m, H$^{3''',4''',5'''}$), 2.40 (3H, s, CH$_3$). – $^{13}$C NMR (500 MHz, CDCl$_3$): δ = 156.4 – 155.1 (3C, s, quat. C's), 152.98 (1C, s, C$^1$), 151.98 (1C, s, quat. C), 149.5 (1C, s, quat. C), 149.1 (1C, s, C$^{6'}$), 139.8 (1C, s, quat. C), 136.9 (1C, s, C$^{4'}$), 135.17 – 136.9.9 (2C, s, quat. C), 130.6 (1C, s, C$^{7''}$), 130.40 (1C, s, phenyl CH), 129.39 (1C, s, C$^{6'''}$), 128.8 (1C, s, quat. C), 128.13 (1C, s, phenyl CH), 127.75 (1C, s, C$^{8''}$), 127.62 (1C, s, C$^{5''}$), 127.64 (1C, s, C$^{5''}$), 127.53 (1C, s, C$^{6''}$), 125.9 (1C, s, phenyl CH), 123.81 (C, s, C$^{5'}$), 122.0 (1C, s, C$^3$), 121.4 (1C, s, C$^{3'}$), 121.2 (1C, s, C$^5$), 117.8 (1C, s, C$^{4''}$), 20.8 (1C, s, CH$_3$). – UV/Vis (MeCN): λ(max) = 234, 253, 282, 292, 314 (π-π*) nm.

### [Chloro{4-(*o*-tolyl)-6-(3''-isoquinoyl)-2,2'-bipyridine}-platinum(II)]hexafluoroantimonate

AgSbF$_6$ (137 mg, 0.400 mmol) was dissolved in acetonitrile (5 mL) and added to a suspension of [Pt(PhCN)$_2$Cl$_2$] (198 mg, 0.400 mmol) in acetonitrile (12 mL). The mixture was refluxed over night under an inert atmosphere, and the resultant precipitate of AgCl was removed by filtration using a 0.45 μm nylon filter membrane on a Millipore filtration unit. An equimolar amount of solid 4-(*o*-tolyl)-6-(3''-isoquinoyl)-2,2'-bipyridine (149 mg, 0.400 mmol) was added to the filtrate, and the mixture was refluxed for an additional 24 h. Once the reflux was complete, the mixture was filtered hot and the solvent partially removed under reduced pressure resulting in the precipitation of [Pt{4-(*o*-tolyl)-6-(3''-isoquinoyl)-2,2'-bipyridine}Cl]SbF$_6$ as a bright-red solid. The product was washed on the frit with copious amounts of diethyl ether and smaller amounts of cold acetonitrile, before drying *in vacuo*. Yield: 0.32 g (94 %). – M. p. dec. > 290 °C. Anal. for C$_{26}$H$_{19}$N$_3$: calcd. C 37.2, H 2.3, N 5.0; found C 37.4, 2.3, 5.2. – IR: ν[4-(*o*-tolyl)isqbipy)] = 698w, 727m, 760vs, 788s, 885w, 905w, 976s, 1037w, 1161w, 1244w, 1285w, 1388m, 1418mw, 1448w, 1477mw, 1556m, 1610s; ν(SbF$_6$) = 656vs cm$^{-1}$. – $^1$H NMR (500 MHz, CDCl$_3$): δ = 9.13 (1H, s, H$^{1''}$), 9.06 (1H, s, H$^{4''}$), 8.66, 8.64 (2H, dd, H$^{3,5}$), 8.48 (2H, m, H$^{3',6'}$), 8.17 (2H, m, H$^{4',8''}$), 7.93 (1H, dt, H$^{6''}$), 7.80 (1H, m, H$^{7''}$), 8.80 (1H, m, H$^{5''}$), 7.95 – 7.51 (5H, m, H$^{5',3''',4''',5''',6'''}$), 2.50 (3H, m, CH$_3$). – $^{13}$C NMR (500 MHz, CDCl$_3$): δ = 158.36, 155.39 – 150.94 (5C, s, quat. C's), 155.13 (1C, s, C$^{1''}$), 150.68 (1C, s, C$^{3'}$), 142.43 (1C, s, C$^{4'}$), 137.68.1 (1C, s, quat. C), 136.10 (1C, s, C$^{6''}$), 135.66 – 135.23 (2C, s, quat. C), 132.18 (1C, s, C$^{7''}$), 131.52 – 127.00 (7C, s, C$^{8'',5'',5',3''',4''',5''',6'''}$), 125.89 (1C, s, C$^{6'}$), 125.59 (1C, s, C$^{4''}$), 124.89 – 124.58 (2C, s, C$^{3,5}$), 20.66 (1C, s, CH$_3$). – MS: *m/z* = 603.0917 [M]$^+$. – UV/Vis (MeCN): λ(max) (ε, M$^{-1}$·cm$^{-1}$) = 216 (37500), 260 (40800), 280 (45110), 310 sh (30700), 325 sh (21650), 345 (12630), 362 (17860), 393 sh (6300) nm.

The [Pt{4-(*o*-tolyl)isqbipy}Cl]SbF$_6$ salt is soluble in CH$_2$Cl$_2$/CHCl$_3$ as the TFPB salt after metathesis with

Table 1. Crystal data and structure refinement details for 4-(*o*-tolyl)-6-(3''-isoquinoyl)-2,2'-bipyridine.

| | |
|---|---|
| Empirical formula | C$_{26}$H$_{19}$N$_3$ |
| $M_r$, g mol$^{-1}$ | 373.46 |
| Crystal size, mm$^3$ | 0.05 × 0.20 × 0.40 |
| $T$, K | 293 |
| $λ$, Å | 0.71073 |
| Crystal system | monoclinic |
| Space group | $P2_1/n$ |
| $a$, Å | 15.183(6) |
| $b$, Å | 8.530(4) |
| $c$, Å | 15.976(6) |
| $β$, deg | 107.281(5) |
| $V$, Å$^3$ | 1976(2) |
| $Z$ | 4 |
| $D_c$, g cm$^{-3}$ | 1.26 |
| $μ$, mm$^{-1}$ | 0.1 |
| $F(000)$, e | 784 |
| $θ$ range, deg | 2 – 32 |
| Refl. collected / independent / $R_{int}$ | 14057 / 3900 / 0.0329 |
| Refl. observed [$I ≥ 2σ(I)$] | 2311 |
| No. refined parameters | 263 |
| Final $R_1$ [$I ≥ 2σ(I)$] / $wR_2$ (all data) | 0.0489 / 0.1438 |
| $Δρ$(max / min), e Å$^{-3}$ | 0.15 / −0.19 |

Na[TFPB]·$n$H$_2$O, where TFPB = tetrakis[3,5-bis(trifluoromethyl)phenyl]borate. The emission spectrum shown in Fig. 3 was obtained in this way. A nitrate salt was used to obtain the solution of the complex used to record the DME glass spectra shown in Fig. 4. This was obtained by dissolving the hexafluoroantimonate salt in acetonitrile and precipitating with excess Bu$_4$N[NO$_3$] in the same solvent.

### Crystallography

The instrument used for the collection of the X-ray intensity data was an Oxford Diffraction Xcalibur 2 CCD 4-circle diffractometer linked to an Oxford Cryostat System. The data were collected using Mo$K_α$ radiation (2.0 kW, 0.71073 Å), 0.75° frame widths, 20 s exposures at a crystal-to-detector distance of 50 mm, and omega 2-$θ$ scans of −54.00 to 60.60° or −54.00 to 60.75° at $θ$ = 30°. The data were reduced with the program CRYSALIS RED [41] using outlier rejection, scan speed scaling, as well as standard Lorentz and polarisation correction factors. The structures were solved with SHELXS-97 [42] using Direct and Patterson Methods with all non-hydrogen atoms refined anisotropically with SHELXL-97 [42] (using WINGX [43] as an interface). Hydrogen atoms were geometrically constrained (C–H = 1.05 Å) using the appropriate AFIX command and refined isotropically with $U_{iso}$ fixed at 1.20 times the equivalent isotropic displacement parameters for a parent $sp^2$ carbon atom, and 1.5 times for a parent $sp^3$ carbon atom. Plots were obtained with ORTEP3 for Windows [44]. Lattice constants, structure refinement details and final discrepancy indices are given in Table 1.

CCDC 791302 contains the supplementary crystallographic data for this paper. These data can be obtained free of charge from the Cambridge Crystallographic Data Centre *via* www.ccdc.cam.ac.uk/data_request/cif.

[1] H.-K. Yip, L.-K. Cheng, K.-K. Cheung, C.-M. Che, *J. Chem. Soc., Dalton Trans.* **1993**, 2933.

[2] T. K. Aldridge, E. M. Stacey, D. R. McMillin, *Inorg. Chem.* **1994**, *33*, 722.

[3] J. A. Bailey, M. G. Hill, R. E. Marsh, V. M. Miskowski, W. P. Schaefer, H. B. Gray, *Inorg. Chem.* **1995**, *34*, 4591.

[4] M. H. Wilson, L. P. Ledwaba, J. S. Field, D. R. McMillin, *Dalton Trans.* **2005**, 2754.

[5] J. S. Field, O. Q. Munro, L. P. Ledwaba, D. R. McMillin, *Dalton Trans.* **2007**, 192.

[6] S. E. Hobert, J. T. Carney, S. D. Cummings, *Inorg. Chim. Acta* **2001**, *40*, 2193.

[7] M. L. Muro, F. N. Castellano, *Dalton Trans.* **2007**, 4659.

[8] D. K. Crites, C. T. Cunningham, D. R. McMillin, *Inorg. Chim. Acta* **1998**, *273*, 346.

[9] S.-E. Lai, M. C. W. Chan, K.-K. Cheung, C. M. Che, *Inorg. Chem.* **1999**, *38*, 4262.

[10] G. Arena, G. Calogero, S. Campagna, L. Monsú Scolaro, V. R. Romeo, *Inorg. Chem.* **1998**, *27*, 2763.

[11] R. Buchner, C. T. Cunningham, J. S. Field, R. J. Haines, D. R. McMillin, *J. Chem. Soc., Dalton Trans.* **1999**, 711.

[12] J. F. Michaelec, S. A. Bejune, D. R. McMillin, *Inorg. Chem.* **2000**, *39*, 2708.

[13] J. F. Michaelec, S. A. Bejune, D. G. Cuttell, G. C. Summerton, J.-A. Gertenbach, J. S. Field, R. J. Haines, D. R. McMillin, *Inorg. Chem.* **2001**, *40*, 2193.

[14] R. Büchner, J. S. Field, R. J. Haines, L. P. Ledwaba, R. McGuire, Jr., D. R. McMillin, O. Q. Munro, *Inorg. Chim. Acta* **2007**, *360*, 1633.

[15] T. Yutaka, I. Mori, M. Kurihara, J. Mizutani, N. Tamai, T. Kawai, M. Irie, H. Nishihara, *Inorg. Chem.* **2002**, *41*, 7143.

[16] M. J. Hannon, P. S. Green, D. M. Fisher, P. J. Derrick, J. L. Beck, S. J. Watt, S. F. Ralph, M. M. Sheil, P. R. Barker, N. W. Alcock, R. J. Price, K. J. Sanders, R. L. Pither, J. Davies, A. Rodger, *Chem. Eur. J.* **2006**, *12*, 8000.

[17] J. S. Field, R. J. Haines, D. R. McMillin, G. C. Summerton, *J. Chem. Soc., Dalton Trans.* **2002**, 1369.

[18] J. S. Field, J.-A. Gertenbach, R. J. Haines, L. P. Ledwaba, N. T. Mashapa, D. R. McMillin, O. Q. Munro, G. C. Summerton, *J. Chem. Soc., Dalton Trans.* **2003**, 1176.

[19] T. J. Wadas, Q.-M. Wang, Y.-J. Kim, C. Flaschenreim, T. N. Blanton, R. Eisenberg, *J. Am. Chem. Soc.* **2004**, *126*, 16841.

[20] P. Du, J. Schneider, W. W. Brennessel, R. Eisenberg, *Inorg. Chem.* **2008**, *47*, 69.

[21] J. S. Field, L. P. Ledwaba, O. Q. Munro, D. R. McMillin, *CrystEngComm* **2008**, *10*, 740.

[22] F. Kröhnke, *Synthesis.* **1976**, 1.

[23] E. C. Constable, A. M. W. Cargill, N. T. Armarodi, V. Balzani, M. Maistric, *Polyhedron* **1992**, *11*, 2707.

[24] E. C. Constable, L. Lewis, M. C. Liptrot, P. R. Raithby, *Inorg. Chim. Acta* **1990**, *178*, 47.

[25] L. P. Ledwaba, O. Q. Munro, K. Stewart, *Acta Crystallogr.* **2009**, *E65*, o376.

[26] D. R. McMillin, J. J. Moore, *Coord. Chem. Rev.* **2002**, *229*, 113.

[27] D. K. C. Tears, D. R. McMillin, *Coord. Chem. Rev.* **2001**, *211*, 195.

[28] K. M.-C. Wong, V. W.-W. Yam, *Coord. Chem. Rev.* **2007**, *251*, 2477.

[29] A. Juris, F. Barigelletti, V. Balzani, P. Belser, A. von Zelewsky, *Inorg. Chem.* **1985**, *24*, 202.

[30] We note the high level of instrument noise, unavoidable in view of having to record at such low concentrations in order to obtain a representative spectrum for the monomer in a frozen glass.

[31] N. A. Larew, A. R. van Wassen, K. E. Wetzel, M. M. Machala, S. D. Cummings, *Inorg. Chim. Acta* **2010**, *63*, 57, and refs. therein.

[32] H.-K. Yip, C.-M. Che, Z.-Y. Zhou, T. C. W. Mak, *Chem. Commun.* **1992**, 1369.

[33] W. B. Connick, R. E. Marsh, P. Schaefer, H. B. Gray, *Inorg. Chem.* **1997**, *36*, 913.

[34] J. S. Field, C. D. Grimmer, O. Q. Munro, B. P. Waldron, *Dalton Trans.* **2010**, *39*, 1558.

[35] M. Kato, *Bull. Chem. Soc. Jpn.*, **2007**, *80*, 287.

[36] V. W.-W. Yam, K. M. C. Wong, N. Zhu, *J. Am. Chem. Soc.* **2002**, *124*, 6506.

[37] A. Shaira, MSc thesis, University of KwaZulu-Natal, Pietermaritzburg, **2010**.

[38] F. Barigelletti, B. Ventura, J.-P. Collin, R. Kayhanian, P. Gaviña, J.-P. Sauvage, *Eur. J. Inorg. Chem.* **2000**, 113.

[39] K. L. Cunningham, C. R. Hecker, D. R. McMillin, *Inorg. Chim. Acta* **1996**, *242*, 143.

[40] F. Liu, K. L. Cunningham, W. Uphues, G. W. Fink, J. Schmolt, D. R. Mcillin, *Inorg. Chem.* **1995**, *34*, 2015.

[41] CRYSALIS RED (version 170), Oxford Diffraction Ltd., Abingdon, Oxford (U. K.) **2003**.

[42] G. M. Sheldrick, SHELXS/L-97, Programs for Crystal Structure Determination, University of Göttingen, Göttingen (Germany) **1997**. See also: G. M. Sheldrick, *Acta Crystallogr.* **1990**, *A46*, 467; *ibid.* **2008**, *A64*, 112.

[43] L. J. Farrugia, WINGX, A MS-Windows System of Programs for Solving, Refining and Analysing Single Crystal X-Ray Diffraction Data for Small Molecules, University of Glasgow, Glasgow, Scotland (U. K.) **2005**. See also: L. J. Farrugia, *J. Appl. Crystallogr.* **1997**, *30*, 565; *ibid.* **1999**, *32*, 837.

[44] C. K. Johnson, M. N. Burnett, ORTEP3, Oak Ridge Thermal Ellipsoid Plot Program for Crystal Structure Illustrations, Rep. ORNL-6895, Oak Ridge National Laboratory, Oak Ridge, TN (USA) **1996**. Windows version: L. J. Farrugia, University of Glasgow, Glasgow, Scotland (U. K.) **1999**. See also: L. J. Farrugia, *J. Appl. Crystallogr.* **1997**, *30*, 565.